Available online at www.sciencedirect.com
SCIENCE DIRECT®
International Journal of Mass Spectrometry 228 (2003) 181–190
International Journal of Mass Spectrometry
www.elsevier.com/locate/ijms

Determining C_2 binding energies from KERDs for C_{80}^+ and C_{82}^+ fullerenes and their endohedrals

Tikva Peres[a], Baopeng Cao[b], Hisanori Shinohara[b], Chava Lifshitz[a,*]

[a] *Department for Physical Chemistry and The Farkas Center for Light Induced Processes, The Hebrew University of Jerusalem, Jerusalem 91904, Israel*
[b] *Department of Chemistry, Nagoya University, Nagoya 464-8602, Japan*

Received 4 November 2002; accepted 14 March 2003

Dedicated to Professor Helmut Schwarz on the occasion of his 60th birthday.

Abstract

Kinetic Energy Release Distributions (KERDs) have been measured for the C_2 evaporation from a series of fullerenes including C_{80}^+ and its endohedral compounds, $Sc_3N@C_{80}^+$ and $Ti_2@C_{80}^+$. We have employed Finite Heat Bath Theory (FHBT) to analyze the measured KERDs and to deduce the C_2 binding energies. We re-evaluated previously measured binding energies for C_{82}^+, $La@C_{82}^+$, and $Tb@C_{82}^+$ in the light of recent findings that fragmentation of fullerene ions proceeds via a very loose transition state. This procedure demonstrates a substantial increase in the binding energy on going from C_{82}^+, to $La@C_{82}^+$ & $Tb@C_{82}^+$. The KERDs for all three ions, C_{80}^+, $Sc_3N@C_{80}^+$, and $Ti_2@C_{80}^+$ are nearly overlapping and the C_2 binding energies are equal within experimental error. The binding energy deduced for C_{80}^+ is surprisingly high. C_{82}^+ on the other hand has nearly the same stability as C_{78}^+. These results indicate that C_{80} is a magic number. The results will be discussed in the light of proposed structures for the various compounds and the reliability of data deduced from KERDs.

Keywords: Kinetic Energy Release Distribution (KERD); Fullerenes; Endohedral fullerenes; Finite Heat Bath Theory (FHBT); Binding energies; Magic numbers

1. Introduction

Schwarz and coworkers [1–3] were the first to demonstrate the inclusion of rare gas atoms within C_{60}^+ and C_{70}^+ through high-energy collision experiments. It is thus appropriate to choose the topic of fullerenes and endohedral fullerenes within this issue of IJMS that is dedicated to Professor Helmut Schwarz. The fullerenes are closed cages with cavities large enough to contain atoms and molecules. Evidence that metal atoms can combine with arc-vaporized carbon atoms to form endohedral metallofullerene molecules [4] was reported shortly after the discovery of fullerene molecules [5]. Endohedral metallofullerenes can be isolated in macroscopic amounts. This was achieved by using laser- or arc-vaporization [6] of graphite/metal composites in helium.

Fullerenes, endohedral fullerenes, and their ions undergo the well-known C_2 elimination reaction:

$$C_{2n} \rightarrow C_{2n-2} + C_2 \quad (1)$$

* Corresponding author. Tel.: +972-2-6585866; fax: +972-2-6522472.
E-mail address: chavalu@vms.huji.ac.il (C. Lifshitz).

1387-3806/$ – see front matter © 2003 Elsevier Science B.V. All rights reserved.
doi:10.1016/S1387-3806(03)00207-0

A most controversial issue over the years has been the C_2 binding energy. We have reviewed this topic [7] as well as the general topic of carbon clusters, including fullerenes and endohedral fullerenes [8]. The problem lies in the analysis of experimental data and the energy–entropy tradeoffs encountered in theoretical modeling. The original model calculations assumed a fairly tight transition state for reaction (2) and led to an upper limit for the binding energy of C_{58}^+–C_2 approximately 7.6 eV. The calculations were redone [9] leading to a re-evaluation of the C_2 binding energy in favor of a value in excess of 9.5 eV. Recent calculations used a very loose transition state for reaction (2) with an activation entropy in excess of $\Delta S^{\#} = 18.8$ eu, Arrhenius pre-exponential A factors as high as $2 \times 10^{20}\ s^{-1}$ and included radiative decay, reaction (3), in the modeling,

$$C_{60}^{*+} \rightarrow C_{58}^+ + C_2 \quad (2)$$

$$C_{60}^{*+} \rightarrow C_{60}^+ + h\upsilon \quad (3)$$

(The star symbol in C_{60}^{*+} denotes internal excitation of the C_{60}^+ ion).

All of the recent experiments favor a high C_2 binding energy, in excess of 10 eV in the neutral and in excess of 9.5 eV in the cation, in agreement with DFT and MP2 calculations [10]. The experiments include Kinetic Energy Release Distributions (KERDs) [11–13], time-resolved KERs [14], time-resolved metastable fractions [9], thermionic emission [15], and quenching of excited ions in a storage ring by radiative cooling [16]. In spite of this agreement between experiment and theory, there is still an ongoing controversy concerning this binding energy (see Fig. 1 of ref. [7]).

Relative dissociation energies of the fullerenes were determined through various experimental and theoretical methods. There is general agreement that C_{58}^+ is less stable than C_{60}^+ and that C_{62}^+ is considerably less stable. However, some results [16] demonstrate a dramatic drop in dissociation energy in going from $n \leq 60$ to $n > 60$ whereas other results [17] find the relative dissociation energies for large fullerenes, with $n > 60$, to be at about the same level as those for $n < 60$. This depends somewhat on the normalization procedure, namely in some studies C_{54}^+ is taken as the ion to which all other data are normalized whereas in others it is C_{60}^+. All experimental results demonstrate C_{60} and C_{70}, as well as to a lesser extent also C_{50}, to be particularly stable ('magic'). Very few experiments were carried out for $n \geq 80$ [17].

Deducing thermochemical information such as binding energies from KERs and KERDs is a well-established procedure [18]. We began measuring kinetic energy releases upon dissociation of endohedral fullerenes several years ago [19] with the aim of determining the C_2 binding energies. The question that was of interest to us was to what extent is the cage stabilized or destabilized upon introduction of the endohedral atom. The early measurements were extended later on [11] to include additional endohedral species. As was already pointed out in a *note added in proof* [11], all the calculated binding energies need to be re-evaluated in view of the very loose transition state of reaction (1) and the analogous reactions for endohedral ions. The present paper is devoted to a re-evaluation of the binding energy data [11,19] for C_{82}^+, La@C_{82}^+, and Tb@C_{82}^+. New results will be presented for C_{80}^+, Ti_2@C_{80}^+, and Sc_3N@C_{80}^+.

2. Experimental

2.1. Preparation and isolation of C_{80} and $Ti_2@C_{80}$

The production and isolation of pure C_{80} and $Ti_2@C_{80}$, respectively, have been published by some of us, previously [20,21]. The titanium endohedral and C_{80} were produced by DC arc discharge. Details of the arc discharge instrument have been described elsewhere [22]. Briefly, the soot containing Ti-metallofullerenes was generated by DC (500 A) arc discharge of titanium carbide/graphite composite rods (size: 15 mm × 15 mm × 300 mm; atomic content of Ti: 0.8%; Toyo Tanso Co.) under 50 Torr of flowing He. The discharge voltage between anode and cathode was carefully set to ~9.5 V by

adjusting the distance between two electrodes. The soot was collected under anaerobic conditions. The mixture of metallofullerenes and empty fullerenes were Soxhlet-extracted from the soot by carbon disulfide [23]. The extraction was not terminated unless no color was discernable. CS_2 was removed from the extract solution and the solid mixture was used for isolation of Ti-metallofullerenes.

The isolation of $Ti_2@C_{80}$ was achieved through the so-called multistage HPLC separation process on two complementary columns. In the first stage, a 5PYE column (Naclai Cosmosil, 25 mm × 250 mm) was used to remove the abundant empty fullerenes (C_{60}, C_{70}, C_{76}, C_{78}, C_{82}, C_{84}, and C_{86}) from the fraction containing $Ti_2@C_{80}$. The saturated toluene solution of the extract mixture was injected into the column for rough separation. Toluene with a flow rate of 15 mL/min was used as a moving phase. The fraction containing $Ti_2@C_{80}$ overlapped with that of C_{88} and was collected for further isolation. In the second stage, a recycling HPLC separation on a Buckyclutcher column (Regis, 20 mm × 500 mm) was employed to completely isolate $Ti_2@C_{80}$. By recycling on the Buckyclutcher column, the saturated solution collected in the first step for four cycles, the $Ti_2@C_{80}$ was isolated from C_{88}.

C_{80} was isolated in a similar fashion. In the first stage, the C_{78} fraction overlapped the C_{80} fraction. By recycling the fraction of C_{78} on the 5PYE column for three times, C_{80} could be isolated.

2.1.1. $Sc_3N@C_{80}$

$Sc_3N@C_{80}$ is well known and its preparation has been achieved some years ago [24]. It is now available commercially. We purchased HPLC-pure samples of $Sc_3N@C_{80}$ from Luna Innovations, Inc., and used them without further purification.

2.2. Mass spectrometry and Mass-analyzed Ion Kinetic Energy spectrometry (MIKEs)

Measurements were performed on a high-resolution double-focusing mass spectrometer of reversed geometry, the VG-ZAB-2F [25,26] running mass spectra as well as using the technique of MIKEs. The endohedral fullerene cations were obtained by ionization of the corresponding neutral samples.

The samples were introduced into the mass spectrometer using the direct insertion probe and evaporated at 400 °C. The electron-impact conditions were as follows: electron ionizing energy, 70 eV; emission current, 5 mA; ion source temperature, 400 °C; resolution, 1100 (10% valley definition). Metastable ion peakshapes were determined by scanning the electrostatic analyzer and using single-ion counting. Ion counting was achieved by a combination of an electron multiplier, amplifier/discriminator, and multichannel analyzer [27]. The experiments were performed at 6–8 kV acceleration voltages and a main beam width of ≤2.5 V. The data were accumulated in a computer-controlled experiment, monitoring the main beam scan, and correcting for the drift of the main beam [26]. The metastable ion peak shapes were mean values of 50–500 accumulated scans.

In a MIKE spectrum recorded in the second field-free region ff2, the decay of fragment ions m_2 produced in the first field-free region ff1 from precursor ions m_1 with $m_1 > m_p$ will also contribute if their apparent mass, $m^* = m_2^2/m_1$, is approximately equal to m_p, the mass of the parent ion whose reaction is being studied. This phenomenon contributes to artifact peaks in MIKE spectra of clusters and fullerenes. This was the case in earlier measurements [11,19] in which carbon cluster and fullerene mixtures were studied. The high purity of the C_{80}, $Sc_3N@C_{80}$, and $Ti_2@C_{80}$ samples employed here ensured that the metastable peak shapes were devoid of contributions from artifacts in the present study.

The product KERDs were determined from the first derivatives of the metastable ion peak shapes [28–30].

3. Data analysis

Unimolecular reactions that possess no reverse activation energies, lead to KERDs that are Boltzmann-like and can be modeled by statistical theories. In the

model-free approach, the KERD is written in the form [11,18]:

$$p(\varepsilon) = \varepsilon^{l} \exp\left(\frac{-\varepsilon}{k_B T^{\ddagger}}\right) \quad (0 < l < 1) \tag{4}$$

where ε is the kinetic energy release, l is a parameter that ranges from zero to unity, k_B is Boltzmann's constant, and $T^{\ddagger}$ is the transition state temperature defined by the average kinetic energy on passing through the transition state. The values of l and $T^{\ddagger}$ are obtained by fitting the experimental KERD with Eq. (4) using non-linear regression. It was found that for fullerene fragmentations l is very close to 0.5. This corresponds to the expected value for the most statistical situation, since the translational density of states is proportional [31] to $\varepsilon^{0.5}$.

The isokinetic bath temperature is defined in Finite Heat Bath Theory (FHBT) [32] as the temperature to which a heat bath should be set so that the canonical rate constant, $k(T_b)$, is equal to the microcanonical rate constant, $k(E)$, sampled in the experiment. The isokinetic bath temperature is given by [33,34]

$$T_b = T^{\ddagger} \frac{\exp(\gamma/C) - 1}{\gamma/C} \tag{5}$$

where C is a dimensionless heat capacity and γ is the Gspann parameter [35]. The binding (or vaporization) energy, ΔE_{vap} and the isokinetic bath temperature are connected via the Trouton relation:

$$\Delta E_{vap} = \gamma k_B T_b \tag{6}$$

The currently acceptable value for the Gspann parameter for the C_2 elimination from fullerenes is greater or equal to 33 [9,18] and a value $\gamma = 33$ has been adopted here also for the endohedral fullerenes.

An alternative method for data analysis can sometimes be adopted if the assumption that $l = 0.5$ is considered to be strictly valid [36]. This holds for fragment ion peaks that are truly Gaussian, the KERD is a three-dimensional Maxwell–Boltzmann distribution, and no discrimination against fragment ions occurs. In this situation, the full-width-at-half-maximum, ΔU, of the MIKE peak (derived by using non-linear least squares fitting techniques, and correcting for the finite width of the parent ion peak), provides a robust measure of the average KER, $\bar{\varepsilon}$, through the relation

$$\bar{\varepsilon} = 2.16 \frac{m_p^2 U_{ac}}{16 m_f (m_p - m_f)} \left(\frac{\Delta U}{U_p}\right)^2 \tag{7}$$

where U_{ac} is the high voltage, U_p is the nominal electric sector field voltage, and m_p and m_f are the masses of the parent ion and fragment ion, respectively [18,37].

Furthermore, in this situation, the transition state temperature, $T^{\ddagger}$, of the reaction is easily derived from $\bar{\varepsilon}$,

$$\bar{\varepsilon} = 1.5 k_B T^{\ddagger} \tag{8}$$

We have applied both of these alternative methods in the present study and the results will be demonstrated to be comparable.

4. Results and discussion

4.1. Mass spectra

The mass spectra of C_{80}, $Ti_2@C_{80}$, and $Sc_3N@C_{80}$ are presented in Figs. 1–3, respectively. They demonstrate a high degree of purity. Whereas C_2 eliminations are observed leading from the C_{80}^+ cation to lower fullerene cations (Fig. 1a), impurities such as C_{84} or C_{82} are negligibly small. This is similarly true for the endohedrals, $Ti_2@C_{80}$ and $Sc_3N@C_{80}$, whose mass spectra were free of $Ti_2@C_{84}$ and $Sc_3N@C_{84}$, respectively, as well of other higher endohedral fullerenes that could lead to artifact peaks in MIKE spectra.

4.2. MIKEs and kinetic energy releases

MIKE scans of the parent ions of C_{80}, $Ti_2@C_{80}$, and $Sc_3N@C_{80}$ were performed on the most intense isotope of the isotopic multiplet of peaks in the mass spectra (Figs. 1–3). The MIKE spectra revealed the following three C_2 elimination reactions:

$$C_{80}^+ \rightarrow C_{78}^+ + C_2 \tag{9}$$

$$Ti_2@C_{80}^+ \rightarrow Ti_2@C_{78}^+ + C_2 \tag{10}$$

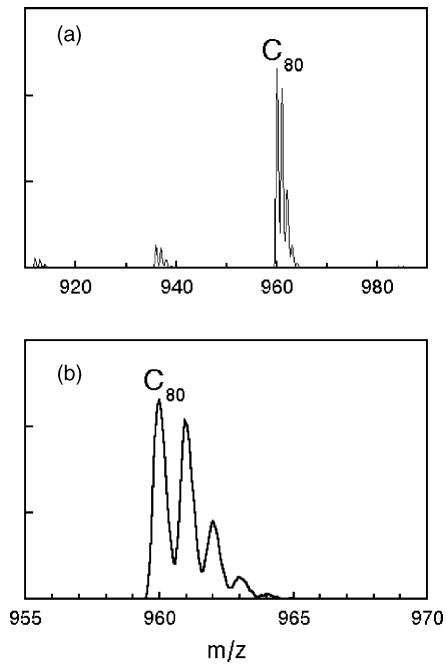

Fig. 1. Positive ion electron-impact (70 eV) mass spectra of C_{80}.

$$Sc_3N@C_{80}^{+} \rightarrow Sc_3N@C_{78}^{+} + C_2 \quad (11)$$

The MIKE spectrum for $Sc_3N@C_{80}^{+}$ is presented in Fig. 4. It contains the narrow parent ion peak in addition to the broad metastable peak both drawn to the same laboratory ion energy scale. The energy broadening in the laboratory scale due to the kinetic energy release in the center of mass (CM) scale of reaction (11) is clearly demonstrated. The metastable peak shape for reaction (9) is represented in Fig. 5 together with the Gaussian fit.

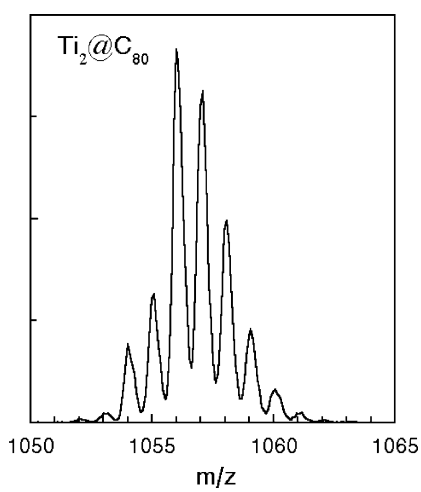

Fig. 2. Mass spectrum of the isotopic multiplet of the parent ion of $Ti_2@C_{80}$.

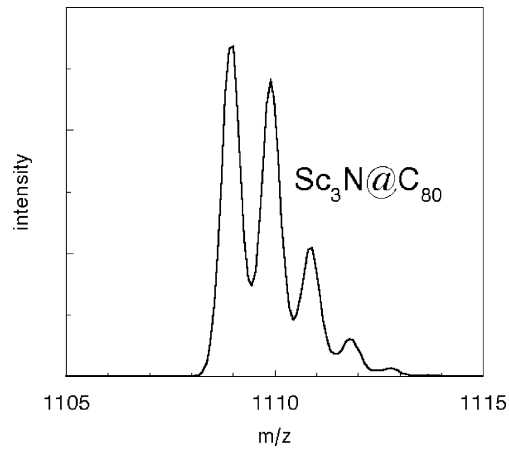

Fig. 3. Mass spectrum of the isotopic multiplet of the parent ion of $Sc_3N@C_{80}$.

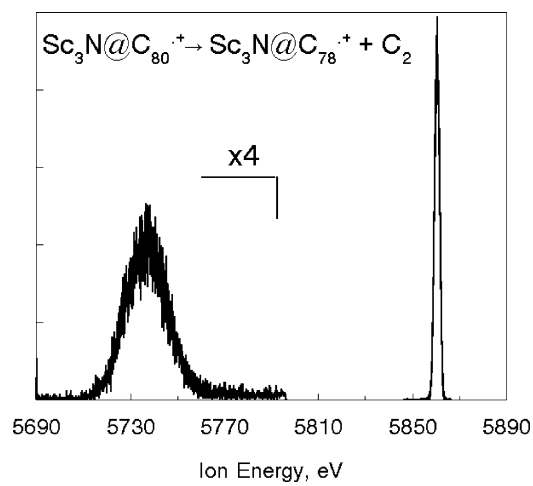

Fig. 4. MIKE spectrum of the parent ion (m/z 1109) of $Sc_3N@C_{80}$. The narrow peak is the parent ion whose maximum is at a laboratory ion energy of 5860.5 eV. The broad peak is due to the metastable ion dissociation, reaction (11), taking place in the second field-free region ff2 of the VG-ZAB-2F instrument.

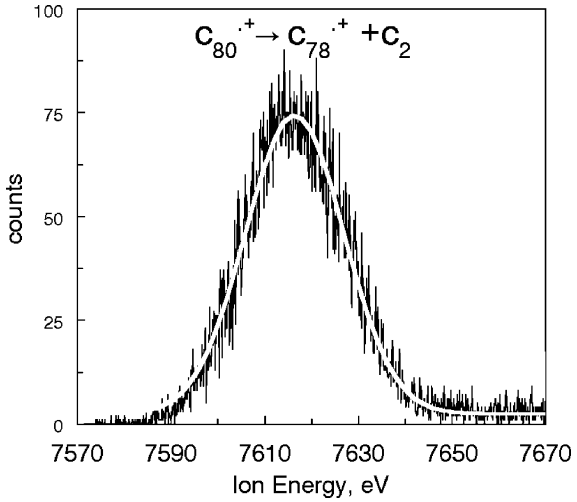

Fig. 5. Metastable ion peak shape for the fragment ion C_{78}^{+} from C_{80}^{+} due to reaction (9) taking place in the second field-free region. The smooth solid line represents a Gaussian fit to the fragment. The parent ion maximum intensity was at 7810.5 eV.

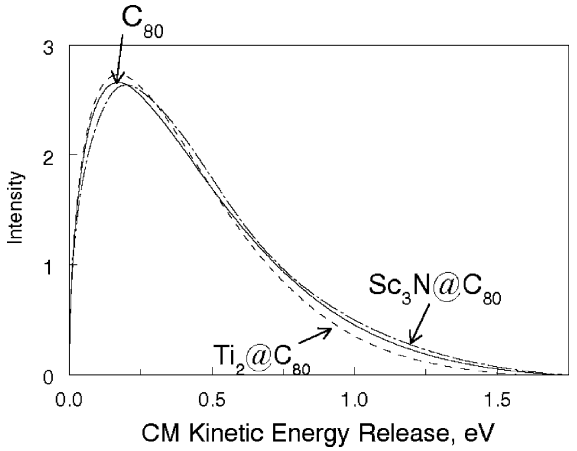

Fig. 7. KERDs in the CM system for reactions (9)–(11); smooth line—reaction (9); dashed line—reaction (10); dash-dotted line—reaction (11).

A typical KERD obtained for reaction (9) is presented in Fig. 6. The modeled KERD (Eq. (4)) is superimposed on the experimental curve (Fig. 6). The parameters of the fitted curve for this experiment are $l = 0.574$ and $T^{\ddagger} = 3419\,\mathrm{K}$. Several experiments of this type under the highest possible energy resolutions were combined and the following results were derived: average kinetic energy release: $\bar{\varepsilon}(9) = 0.46 \pm 0.01\,\mathrm{eV}$; transition state temperature: $T^{\ddagger}(9) = 3500 \pm 270\,\mathrm{K}$; parameter: $l = 0.60 \pm 0.09$. The alternative method of deriving the transition state temperature from the width at half height of the fitted metastable peak (Fig. 5) gave $T^{\ddagger}(9) = 3560 \pm 80\,\mathrm{K}$.

The KERDs derived for all three reactions (reactions (9)–(11)) are nearly super-imposable, (Fig. 7).

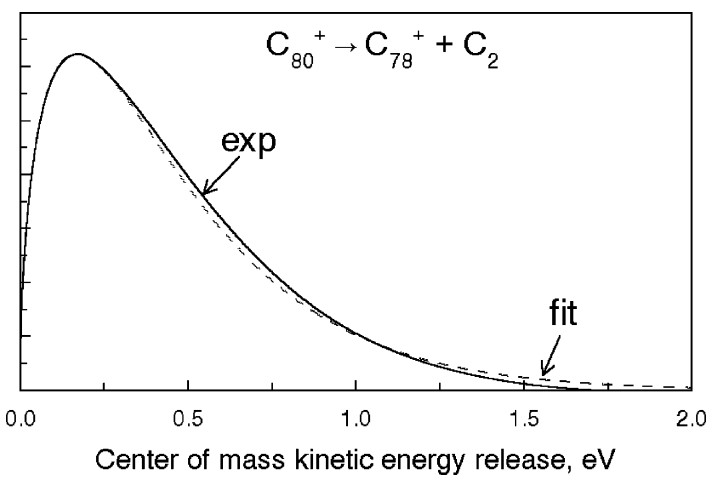

Fig. 6. Kinetic energy release distribution (KERD) in the CM system deduced from the metastable peak shape for reaction (9); smooth curve—experimental; dashed line—fit based on Eq. (4). See the text for further details.

Table 1
Modeling results for fullerenes and metallofullerenes

	$\bar{\varepsilon}$ (eV)	$T^{\ddagger}$ (K)	T_b (K)	$\Delta E'_{vap}$ (eV)	$\Delta E''_{vap}$ (eV)
C_{80}^+	0.46 ± 0.01	3500[a]	3760	10.69[b]	9.4[c]
$Ti_2@C_{80}^+$	0.43 ± 0.02	3360[a]	3600	10.23[b]	9.0[c]
$Sc_3N@C_{80}^+$	0.50 ± 0.05	3470[a]	3715	10.56[b]	9.3[c]
C_{82}^+	0.35 ± 0.02	2860[d]	3065	8.72[e]	8.5[c]
$La@C_{82}^+$	0.46 ± 0.02	3620[d]	3875	11.02[e]	10.7[c]
$Tb@C_{82}^+$	0.55 ± 0.02	4650[d]	4980	14.2[e]	13.8[c]

[a] Present data derived from the KERDs.
[b] Present results using $\gamma = 33$.
[c] Data from previous column re-normalized to a binding energy of 10 eV for C_{60}^+. The present data were normalized by a factor 10/11.3 whereas the previous data from ref. [11] were normalized by the corresponding factor relevant to those experiments, namely 10/10.3.
[d] Data from ref. [11] derived from the corresponding KERDs.
[e] Results from ref. [11] re-calculated using $\gamma = 33$.

The parameters deduced from the KERDs are summarized in Table 1.

In addition to the reactions of C_{80}^+ and its two endohedrals studied here, we have recalculated data from reference [11] concerning reactions of C_{82}^+ and two of its endohedrals,

$$C_{82}^+ \rightarrow C_{80}^+ + C_2 \quad (12)$$

$$La@C_{82}^+ \rightarrow La@C_{80}^+ + C_2 \quad (13)$$

$$Tb@C_{82}^+ \rightarrow Tb@C_{80}^+ + C_2 \quad (14)$$

The average energies and transition state temperatures ($T^{\ddagger}$) deduced from the KERDs [11] are included in Table 1.

4.3. Binding energies

We have obtained for reaction (2) in C_{60}, $T^{\ddagger}(2) = 3600$ K and $l = 0.50$. Using Eqs. (5) and (6) with the preferred Gspann parameter for reaction (2), $\gamma(2) = 33$ and the experimental kinetic energy release data for reaction (2), gives $\Delta E_{vap}(C_{60}^+) = 11.3$ eV. This value is somewhat higher but within error limits of previous determinations [7,13,38] of the binding energy of C_2 in C_{60}^+. Applying similarly the FHBT equations to the KERD data for reactions (9)–(11) gives:

$\Delta E_{vap}(C_{80}^+) = 10.7 \pm 0.8$ eV; $\Delta E_{vap}(Ti_2@C_{80}^+) = 10.2 \pm 1.1$ eV; $\Delta E_{vap}(Sc_3N@C_{80}^+) = 10.6 \pm 0.7$ eV. Re-normalizing the new data for C_{80}^+ and its endohedrals to the traditional value $\Delta E_{vap}(C_{60}^+) = 10$ eV [16], we obtain:

$\Delta E_{vap}(C_{80}^+) = 9.4 \pm 0.7$ eV; $\Delta E_{vap}(Ti_2@C_{80}^+) = 9.0 \pm 1$ eV; $\Delta E_{vap}(Sc_3N@C_{80}^+) = 9.3 \pm 0.6$ eV.

In addition, we have used the previously published data for $T^{\ddagger}$ for reactions (12)–(14) (Table 1) to recalculate binding energies using $\gamma = 33$. The experiments that were run at the time [11] gave $T^{\ddagger}(2) = 3300$ K and the results for C_{82}^+, $La@C_{82}^+$, and $Tb@C_{82}^+$ were normalized to the corresponding C_2 binding energy of C_{60}^+ accordingly. The results are as follows:

$\Delta E_{vap}(C_{82}^+) = 8.5 \pm 0.4$ eV; $\Delta E_{vap}(La@C_{82}^+) = 10.7 \pm 0.5$ eV; $\Delta E_{vap}(Tb@C_{82}^+) = 13.8 \pm 0.5$ eV.

All of the results are summarized in Table 1. The binding energies for C_{80}^+ and C_{82}^+ and their endohedrals are represented in Fig. 8.

Several conclusions transpire from the data:

1. The C_2 binding energies of C_{80}^+ and its endohedrals are equal within experimental error.
2. The C_2 binding energies of C_{82}^+ and its endohedrals are very different. There is a pronounced increase in the binding energy upon introduction of the La atom into the cage and a further increase upon the introduction of Tb.
3. The C_2 binding energy of empty C_{80}^+ is slightly higher than that of C_{82}^+.

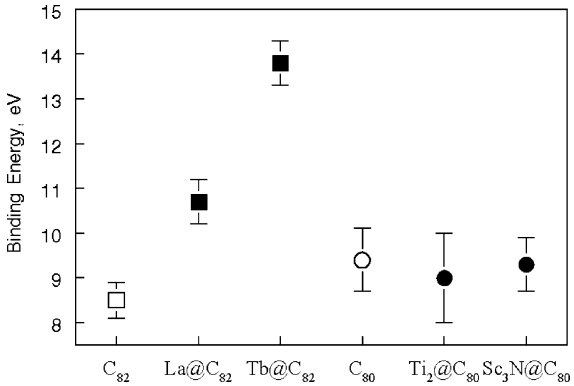

Fig. 8. C_2 binding energies in eV for empty fullerenes (open symbols) and endohedral fullerenes (filled symbols); squares—C_{82} and its metallofullenes; circles—C_{80} and its metallofullerenes.

4.4. The relative stabilities of C_{80}, C_{82}, and their endohedrals

It has been pointed out [39] that nature prefers to generate metallofullerenes with chemically reactive fullerene isomers. Accepting one or more electrons from the encapsulated metal atoms stabilizes these fullerene isomers. Indeed, the isolable metallofullerenes studied here employ unstable isomers of C_{80} and C_{82} as carbon cages. For the C_{80} fullerene, there are seven distinct isomers that satisfy the isolated pentagon rule [40]. The two most stable isomers that are of nearly equal stability have D_2 and D_{5d} symmetries, the first being the major isomer and the second the minor one. These are the isomers that have been isolated by Kappes and coworkers [41] and by Shinohara and coworkers [20], respectively, and characterized by UV-Vis NIR and ^{13}C NMR spectroscopy. We have employed, in this study, a sample of the D_2 isomer. The metallofullerenes stabilize the I_h isomer that is the least stable one among all the empty C_{80} isomers. This is the structure adopted by $Sc_3N@C_{80}$ [24]. Two isomers of $Ti_2@C_{80}$ have been produced, with D_{5h} and I_h symmetries, respectively [21], but they have not been separated. We have employed a mixture in which the D_{5h} isomer is dominant (75–80%) as opposed to the I_h isomer (20–25%). These kinetically stable metallofullerenes are made from empty fullerene cages that are highly unstable kinetically [39]. Our present results based on the kinetic energy release measurements demonstrate that the I_h and D_{5h} cages have been stabilized by the Sc_3N and Ti_2 endohedrals to the empty C_{80} (D_2) level.

Shinohara [23] reviewed recently the chemistry and physics of endohedral metallofullerenes. He pointed out [23] that C_{80} (I_h) has only two electrons in the four-fold degenerate highest occupied molecular orbital (HOMO) level and can accommodate six more electrons to form the stable closed-shell electronic state with a large HOMO–LUMO gap. The Sc_3N unit donates six electrons to the C_{80} (I_h) cage forming $(Sc_3N)^{6+}@C_{80}{}^{6-}$. The situation regarding $Ti_2@C_{80}$ is less clear-cut. Its electronic structure has been discussed [21]. Electronic energy loss spectroscopy (EELS) has demonstrated that the valence state of titanium within $Ti_2@C_{80}$ is slightly lower than +2 [21], in other words that the total number of transferred electrons is four (or a bit less than four), suggesting $Ti_2{}^{4+}@C_{80}{}^{4-}$. Theoretical calculations using a bond resonance energy (BRE) model shows the electronic structure of $Ti_2@C_{80}$ (D_{5h}, the major isomer in this study) is $(Ti^+)_2@C_{80}{}^{2-}$ and there may be some covalent interaction between Ti_2 and the C_{80} (I_h) cage [39]. This means that the evidence is not in favor of donation of six electrons to the C_{80} cage in this case.

The relative stability of negatively charged cages is of great help as an index for predicting the most favorable carbon cage [42]. The C_{82} fullerene has nine isomers that satisfy the isolated pentagon rule but only the most stable one with C_2 symmetry has been produced. A three-electron transfer from La to the C_{82} cage forming $La^{3+}@C_{82}{}^{3-}$ markedly changes the relative stability of the isomers [42] and two isomers with C_{2v} and C_s symmetry, respectively, have been isolated [43–45]. Whereas neutral $La@C_{82}$ has an open-shell structure and is paramagnetic, most neutral C_{80} endohedral fullerenes are closed-shell species. $Ti_2@C_{80}$ has been termed ‘an exceptional metallofullerene’ [39]. Because of the non-closed shell structure for the I_h isomer of $Ti_2@C_{80}$ its stability is much less than that of the D_{5h} isomer. Further studies are needed in order to decide whether these

differences affect the relative stabilities of the corresponding singly charged positive ions.

Most importantly from our point of view, is the fact that $La@C_{82}$ and $La_2@C_{80}$ have been isolated [23] but $La@C_{80}$ is unstable and has not yet been isolated. On the other hand, in addition to $Sc_3N@C_{80}$ being a very stable and isolable endohedral fullerene, the compound $Sc_3N@C_{78}$ has also been isolated and characterized [46]. We assume that the relative stability of these endohedral fullerenes does not change dramatically upon ionization and formation of the corresponding singly charged positive ions. As a result, reaction (11), the C_2 elimination from $Sc_3N@C_{80}^+$, produces a rather stable product ion, $Sc_3N@C_{78}^+$ whose neutral counterpart has been isolated. This is in line with the relatively low binding energy of $Sc_3N@C_{80}^+$ that is comparable to that of the empty cage C_{80}^+ ion. Furthermore, the very high binding energy of $La@C_{82}^+$ deduced for reaction (13) is in line with the instability of $La@C_{80}^+$ as judged on the basis of the instability of its neutral counterpart. The C_2 binding energies of the endohedral metallofullerenes that we have deduced thus reflect the stabilities of the electronic structures of the corresponding reactant and product cages.Previous studies [17,41,47] have shown that C_{80} is less stable than either C_{78} or C_{82}. We find that the C_2 binding energy of C_{82}^+ is $\Delta E_{vap}(C_{82}^+) = 8.5 \pm 0.4$ eV. This value is equal to the one obtained for C_{78}^+ by Tomita et al. [16]. However, the value we obtain for C_{80}^+ is higher than the other two, $\Delta E_{vap}(C_{80}^+) = 9.4 \pm 0.7$ eV. Our present data seem to indicate that contrary to previous beliefs, based partly on C_{80} being a "missing" fullerene [41] and very difficult to isolate, it is not less stable than its neighbors but rather more stable. If this is indeed the case, it could be the result of ionizing directly the most stable neutral C_{80} isomer rather than obtaining the C_{80}^+ ion from consecutive dissociations of higher fullerenes. The reaction cascade leading by consecutive C_2 elimination could conceivably form an isomer that is less stable than the one formed by us when ionizing the D_2 isomer. T.D. Märk (personal communication, September 2002) is now in the process of re-measuring the C_2 binding energies of the fullerene cations for a wide range of sizes using the method of kinetic energy releases described here. He has found $\Delta E_{vap}(C_{80}^+) = 9.38 \pm 0.07$ eV and $\Delta E_{vap}(C_{82}^+) = 8.58 \pm 0.03$ eV in excellent agreement with our data and with considerably lower error bars.

Acknowledgements

The research is part of the European Commission 5th Framework Program "Delayed ionization and competing cooling mechanisms in atomic clusters" (Cluster Cooling, HPRN-CT-2000-00026). C.L. thanks the Austrian Friends of The Hebrew University and Professor Tilmann Märk for financial support and scientific collaboration. The Farkas Research Center is supported by the Minerva Gesellschaft für die Forschung GmbH München. H.S. thanks the JSPS for the Program on New Carbon Nano-Materials and Special Coordination Funds of the Ministry of Education, Culture, Sports, Science, and Technology for the financial support.

References

[1] T. Weiske, D.K. Böhme, J. Hrusák, W. Krätchmer, H. Schwarz, Angew. Chem. Int. Ed. 30 (1991) 884.
[2] T. Weiske, J. Hrusák, D.K. Böhme, H. Schwarz, Helv. Chim. Acta 75 (1992) 79.
[3] T. Weiske, T. Wong, W. Krätchmer, J.K. Terlouw, H. Schwarz, Angew. Chem. Int. Ed. 31 (1992) 183.
[4] J.R. Heath, S.C. O'Brien, Q. Zhang, Y. Liu, R.F. Curl, H.W. Kroto, F.K. Tittel, R.E. Smalley, J. Am. Chem. Soc. 107 (1985) 7779.
[5] H.W. Kroto, J.R. Heath, S.C. O'Brien, R.F. Curl, R.E. Smalley, Nature 318 (1985) 162.
[6] (a) Y. Chai, T. Guo, C. Jin, R.E. Haufler, L.P.F. Chibante, J. Fure, L. Wang, J.M. Alford, R.E. Smalley, J. Phys. Chem. 95 (1991) 7564;
(b) R.D. Johnson, M.S. de Vries, J.R. Salem, D.S. Bethune, C.S. Yanoni, Nature 355 (1992) 239.
[7] C. Lifshitz, Int. J. Mass Spectrom. 198 (2000) 1.
[8] C. Lifshitz, Int. J. Mass Spectrom. 200 (2000) 423.
[9] J. Laskin, B. Hadas, T.D. Märk, C. Lifshitz, Int. J. Mass Spectrom. 177 (1998) L9.
[10] A.D. Boese, G.E. Scuseria, Chem. Phys. Lett. 294 (1998) 233.
[11] J. Laskin, T. Peres, A. Khong, H.A. Jiménez-Vázquez, R.J. Cross, M. Saunders, D.S. Bethune, M.S. de Vries, C. Lifshitz, Int. J. Mass Spectrom. Ion Processes 185–187 (1999) 61.

[12] S. Matt, M. Sonderegger, R. David, O. Echt, P. Scheier, J. Laskin, C. Lifshitz, T.D. Märk, Int. J. Mass Spectrom. Ion Processes 185–187 (1999) 813.
[13] S. Matt, O. Echt, M. Sonderegger, R. David, P. Scheier, J. Laskin, C. Lifshitz, T.D. Märk, Chem. Phys. Lett. 303 (1999) 379.
[14] S. Matt, R. Parajuli, A. Stamatovic, P. Scheier, T.D. Märk, J. Laskin, C. Lifshitz, Eur. Mass Spectrom. 5 (1999) 477.
[15] K. Hansen, O. Echt, Phys. Rev. Lett. 78 (1997) 2337.
[16] S. Tomita, J.U. Andersen, C. Gottrup, P. Hvelplund, U.V. Pedersen, Phys. Rev. Lett. 87 (2001) 073401.
[17] P.E. Barran, S. Firth, A.J. Stace, H.W. Kroto, K. Hansen, E.E.B. Campbell, Int. J. Mass Spectrom. Ion Processes 167/168 (1997) 127.
[18] J. Laskin, C. Lifshitz, J. Mass Spectrom. 36 (2001) 459.
[19] J. Laskin, H.A. Jimenez-Vazquez, R. Shimshi, M. Saunders, M.S. de Vries, C. Lifshitz, Chem. Phys. Lett. 242 (1995) 249.
[20] C.-R. Wang, T. Sugai, T. Kai, T. Tomiyama, H. Shinohara, Chem. Commun. (2000) 557.
[21] B. Cao, M. Hasewaga, K. Okada, T. Tomiyama, T. Okazaki, K. Suenaga, H. Shinohara, J. Am. Chem. Soc. 123 (2001) 9679.
[22] T.J.S. Dennis, H. Shinohara, Appl. Phys. A 66 (1998) 243.
[23] H. Shinohara, Rep. Prog. Phys. 63 (2000) 843.
[24] S. Stevenson, G. Rice, T. Glass, K. Harich, F. Cromer, M.R. Jordan, J. Craft, E. Hadju, R. Bible, M.M. Olmstead, K. Maitra, A.J. Fisher, A.L. Balch, H.C. Dorn, Nature 401 (1999) 55.
[25] P.P. Morgan, J.H. Beynon, R.H. Bateman, B.N. Green, Int. J. Mass Spectrom. Ion Phys. 28 (1978) 171.
[26] N.J. Kirshner, M.T. Bowers, J. Phys. Chem. 91 (1987) 2573.
[27] C. Lifshitz, F. Louage, J. Phys. Chem. 93 (1989) 6533.
[28] J.L. Holmes, A.D. Osborne, Int. J. Mass Spectrom. Ion Phys. 23 (1977) 189.
[29] C. Lifshitz, E. Tzidony, Int. J. Mass Spectrom. Ion Phys. 39 (1981) 181.
[30] M.F. Jarrold, W. Wagner-Redeker, A.J. Allies, N.J. Kirchner, M.T. Bowers, Int. J. Mass Spectrom. Ion Processes 58 (1984) 63.
[31] (a) R.D. Levine, R.B. Bernstein, Molecular Reaction Dynamics and Chemical Reactivity, Oxford University, New York, 1987, pp. 274–275;
(b) T. Baer, W.L. Hase, Unimolecular Reaction Dynamics, Oxford University, New York, 1996, pp. 173–174;
(c) P. Urbain, F. Remacle, B. Leyh, J.C. Lorquet, J. Phys. Chem. 100 (1996) 8003.
[32] C.E. Klots, J. Chem. Phys. 90 (1989) 4470.
[33] Lifshitz, C., in: T. Baer, C.Y. Ng, I. Powis (Eds.), Current Topics in Ion Chemistry and Physics: Clusters, Wiley, New York, 1993.
[34] C.E. Klots, Z. Phys. D 21 (1991) 335.
[35] C.E. Klots, Int. J. Mass Spectrom. Ion Processes 100 (1990) 457.
[36] S. Matt-Leubner, A. Stamatovic, R. Parajuli, P. Scheier, T.D. Märk, O. Echt, C. Lifshitz, Int. J. Mass Spectrom. 222 (2003) 213.
[37] J.L. Holmes, J.K. Terlouw, Org. Mass Spectrom. 15 (1980) 383.
[38] B. Cao, T. Peres, R.J. Cross Jr., M. Saunders, C. Lifshitz, J. Phys. Chem. A 105 (2001) 2142.
[39] J.-I. Aihara, J. Phys. Chem. A 106 (2002) 11371.
[40] K. Kobayashi, S. Nagase, T. Akasaka, Chem. Phys. Lett. 245 (1995) 230.
[41] F.H. Hennrich, R.H. Michel, A. Fischer, S. Richard-Schneider, S. Gilb, M.M. Kappes, D. Fuchs, M. Bürk, K. Kobayashi, S. Nagase, Angew. Chem. Int. Ed. Engl. 35 (1996) 1732.
[42] K. Kobayashi, S. Nagase, Chem. Phys. Lett. 282 (1998) 325.
[43] R.D. Johnson, M.S. de Vries, J. Salem, D.S. Bethune, C.S. Yannoni, Nature 355 (1992) 239.
[44] T. Akasaka, T. Wakahara, S. Nagase, K. Kobayashi, M. Waelchli, K. Yamamoto, M. Kondo, S. Shirakura, s. Okubo, Y. Maeda, T. Kato, M. Kako, Y. Nakadaira, R. Nagahata, X. Gao, E. Van Caemelbecke, K.M. Kadish, J. Am. Chem. Soc. 122 (2000) 9316.
[45] T. Akasaka, T. Wakahara, S. Nagase, K. Kobayashi, M. Waelchli, K. Yamamoto, M. Kondo, S. Shirakura, Y. Maeda, T. Kato, M. Kako, Y. Nakadaira, X. Gao, E. Van Caemelbecke, K.M. Kadish, J. Phys. Chem. 105 (2001) 2971.
[46] M.H. Olmstead, A. de Bettencourt-Dias, J.C. Duchamp, S. Stevenson, D. Marciu, H.C. Dorn, A.L. Balch, Angew. Chem. Int. Ed. 40 (2001) 1223.
[47] R.D. Beck, J. Rockenberger, P. Weis, M.M. Kappes, J. Chem. Phys. 104 (1996) 3638.